Increased interfacial thickness of the NaF, NaCl and NaBr salt aqueous solutions probed with non-resonant surface second harmonic generation (SHG)

ARTICLE *in* PHYSICAL CHEMISTRY CHEMICAL PHYSICS · AUGUST 2008

Impact Factor: 4.49 · DOI: 10.1039/b806362a · Source: PubMed

5 AUTHORS, INCLUDING:

Yuan Guo
Chinese Academy of Sciences
37 PUBLICATIONS **590** CITATIONS
SEE PROFILE

Hong-fei Wang
Pacific Northwest National Laboratory
56 PUBLICATIONS **1,708** CITATIONS
SEE PROFILE

Increased interfacial thickness of the NaF, NaCl and NaBr salt aqueous solutions probed with non-resonant surface second harmonic generation (SHG)

Hong-tao Bian,† Ran-ran Feng,† Yan-yan Xu,† Yuan Guo and Hong-fei Wang*

Received 15th April 2008, Accepted 3rd June 2008
First published as an Advance Article on the web 20th June 2008
DOI: 10.1039/b806362a

Specific ion effects on the nonlinear optical response from the water molecules at the air/sodium halide solution interfaces are measured using non-resonant surface second harmonic generation (SHG). Procedures have been developed to monitor and remove the impurities in the salt solution samples to ensure measurement of small changes in the SHG signal. Quantitative polarization analysis of the measured SHG data indicated that the average orientation of the interfacial water molecules changed only slightly around 40° with the increase of the bulk concentration of the three sodium halides, namely NaF, NaCl and NaBr, from that of the neat air/water interface. The observed significant SHG signal increase with the bulk salt concentration is attributed to the overall increase of the thickness of the interfacial water molecular layer, following the order of NaBr > NaCl ≈ NaF. The absence of the electric-field-induced SHG (EFISHG) effect indicated that the electric double layer at the salt aqueous solution interface is much weaker than that predicted from the molecular dynamics (MD) simulations. These results provided quantitative data to the specific anion effects on the interfacial water molecules of the electrolyte aqueous solution, not only for the larger and more polarizable Br^- anion, but also for the smaller and less polarizable F^- and Cl^- anions.

I. Introduction

Characterization of the surface structure of the aqueous electrolyte solution at the molecular level has recently attracted extensive attention. Recent interest in atmospheric chemistry research, as well as the development of molecular dynamics (MD) simulation capabilities and the rapid development of the surface-sensitive probing techniques have provided new tools and novel understandings.[1–18] In these efforts, particular interest has been given to specific interfacial ion effects.[7,19] There are two fundamental questions, and both of them are yet to reach definite conclusions.[2–6] One is whether the ions, or to be more specific, the anions can be enriched at the interfacial region of an electrolyte aqueous solution. The other is how the interfacial water molecules are influenced by the presence of particular ions in the vicinity of the interface.

Ions have long been considered to be depleted from the surface of an aqueous solution of simple electrolytes, such as the alkali halides.[20–22] According to the Gibbs adsorption equation, the increase of the surface tension of water with the addition of simple inorganic salts was explained by the assertion that the simple ions can only have a "negative adsorption" at the aqueous interface.[22] The subsequent electrostatic theory incorporated with the image charge repulsion effect, *i.e.* the Wagner–Onsager–Samaras model, provided a quantitative molecular theory for the ion (both anion and cation) depletion picture for the aqueous interface at low electrolyte concentration.[21,23]

Such a classical picture remained unchallenged till the 1990s. Photoelectron experiments[24,25] and molecular dynamic simulations[26–28] showed that the halide anions tend to reside on the surface of small water clusters. Results on the chemical reaction occurring on aqueous sea-salt particles and ocean surfaces also indicated a likely incompatibility with the picture of an ion-free aqueous surface.[10,13,29] Recent MD simulations on the aqueous systems, especially the development of the polarizable force fields of liquid water molecules, predicted specific anion effects at the interface of simple electrolyte aqueous solutions.[4,5] These studies predicted the enrichment effect of the halide anions in the aqueous solution interfacial region, and also pointed out that the enrichment is associated with the electrostatic polarizability of the specific anions.[15] For example, the concentration of I^- in the interfacial region can be as high as three times that for the 1.2 M NaI solution. To verify this prediction, direct experimental measurement of the aqueous solution interface were conducted with X-ray photoelectron spectroscopy (XPS),[14] X-ray fluorescence[30] and interface specific nonlinear optical spectroscopy techniques,[31,32] namely the resonant second harmonic generation (resonant SHG)[6,33–38] and the sum-frequency generation vibrational spectroscopy (SFG-VS).[8,9,39–41] These experiments confirmed the presence of the more polarizable anions at aqueous interfaces, and their increasing influence on hydrogen bonding structure in the interfacial region was

Beijing National Laboratory for Molecular Sciences, State Key Laboratory of Molecular Reaction Dynamics, Institute of Chemistry, Chinese Academy of Sciences, Beijing, China 100190.
E-mail: hongfei@iccas.ac.cn; Fax: +86 (0)10 6256 3167; Tel: +86 (0)10 6255 5347
† Also Graduate University of the Chinese Academy of Sciences.

also observed. However, a few experiments also disagreed with this picture.[9,42]

To our knowledge, the measurement of the SCN^- SFG vibrational spectra at the air/KSCN salt solution interface provided the only direct evidence supporting the adsorption of the large, polarizable inorganic anions at the air/aqueous interface so far.[40,41] However, there is still no consensus regarding the magnitude of the enhancement of surface concentration relative to the bulk,[43] even though some of the recent MD simulation results and the resonant SHG measurements indicated a significant enrichment for some large and polarizable anions.[4,6]

Shen and Shultz's group first probed the surface O–H stretch vibration of inorganic salt and acid solution interfaces with interface selective SFG vibrational spectroscopy.[2,39,44–46] Various other systems have been investigated since, including acid, base, salt and other small ion solutions.[3,8,9,47] Among them, the O–H stretching vibrational spectra of the sodium halide aqueous solution interface have been of particular interest,[3,8,9] because these are the simplest systems to exemplify the specific anion effects on aqueous solution interfaces.[7,19] By adding NaF, NaCl, NaBr and NaI salt into water at different concentrations, the spectral features in the O–H stretching SFG vibrational spectra (in the ssp polarization combinations) of the interfacial water species were influenced differently. The O–H stretching vibration SFG-VS spectra of the neat air/water interface has been extensively studied in the literature.[44,48–52]

The two SFG-VS experimental measurements on the O–H stretching vibrational spectra of the sodium halide aqueous solution interface agreed qualitatively.[3,8,9] The narrow peak around 3700 cm^{-1} which corresponds to the O–H stretching vibration of the "free" O–H bond at the air/water interface was not perturbed with different salts at different concentrations up to about 2 M; the broad peak around 3400 cm^{-1} and 3200 cm^{-1} which correspond to the stretching vibration of the hydrogen bonded water species in the vicinity of the air/water interface clearly showed specific anion effects. Particularly, the NaBr and NaI salts significantly increased the intensity of the broad 3400 cm^{-1} band, and slightly decreased the intensity of the broad 3200 cm^{-1} band, with the larger and more polarizable I^- anion exerting the largest influence. A relatively small and broad spectral feature also emerged above the 3700 cm^{-1} narrow band with the increase of the sodium halide salts concentration. This increase followed the order of NaF < NaCl < NaBr < NaI. These observations confirmed the presence of anions, particularly the larger and more polarizable anions, in the interfacial region.

Nevertheless, there were different observations and interpretations in the details of the SFG-VS experimental data.

In Allen *et al.*'s SFG-VS spectra in the ssp polarization combination, the intensity of the broad 3400 and 3200 cm^{-1} bands of the 0.83 M (0.015 molar fraction) NaF solution is essentially the same as that of the neat air/water interface; while in Richmond *et al.*'s data, the intensity of these two bands of the 0.88 M (0.016 molar fraction) NaF solution is about 30% lower than that of the neat air/water interface.[8,9] Thus the former concluded that there was an insignificant F^- anion effect, in good agreement with the MD simulation results that the small and much less polarizable F^- anion was repelled from the air/water interface; while the latter concluded that the reduction of the band intensity was due to the enhancement of the hydrogen bonding network in the interface region by the F^- anion. SFG-VS experiments in our laboratory quantitatively reproduced the SFG-VS spectra as reported by Richmond *et al.* We also observed a clear and gradual decrease of the 3400 and 3200 cm^{-1} band intensity from the 0.2 M up to the 0.9 M NaF solution. This means that the specific F^- anion effect does exist and cannot be neglected. These SFG-VS results will be reported elsewhere.

Another divergence in the interpretation is on the thickness or depth of the interfacial water molecular layer, according to Allen *et al.*, by comparing the Raman and infrared measurements of the bulk solutions and their interfacial SFG (ssp polarization combination) spectral intensities in the O–H stretching vibration region. The increase of the SFG intensity in the broad 3400 cm^{-1} band region for the NaBr and NaI salt solution interfaces was attributed to the increase of the thickness or depth of the interfacial water layers,[3,8] while for the NaF and NaCl salt solutions, such a change of the interfacial thickness or depth from that of the neat air/water interface was not observed. However, Richmond *et al.* pointed out that it is rather difficult to quantify the number of water molecules and/or ions in the interfacial region because the SFG spectral intensity is the convoluted effect of the number of interfacial molecules, their orientations and transition moments.[9]

In addition, according to Richmond *et al.*'s SFG data of the $HOD/H_2O/D_2O$ mixture halide aqueous solution interfaces, it is not likely that there is any significant enrichment of ions, even of the larger and more polarizable anions, over their bulk concentrations.[9] This last conclusion is in direct disagreement with MD simulations, X-ray photoelectron spectroscopy measurements, as well as resonant SHG measurements of halide aqueous solution interfaces.[4,6,14] A recent X-ray reflectivity study on the interface of a series of simple salt solutions also contradicted the picture of the enrichment of the interfacial anions.[42]

Regarding the issue on whether the interfacial thickness or depth of the aqueous salt solution changes or not, polarization dependent non-resonant second harmonic generation (SHG) is the technique that may provide quantitative answers. The interface can be defined as the entity wherever the inversion symmetry is broken.[3,31,53] Unlike the SFG-VS, which measures the spectral resolved features of the different interfacial chemical species, non-resonant SHG measures the overall or total SHG response from the chemical species in the whole interfacial region. In the non-resonant SHG, the contribution to the SHG signal from the interfacial ions can be neglected, as the hydrated ions can be assumed to be centrosymmetric. Therefore, non-resonant SHG is the direct measurement of the water species in the whole interfacial region for the electrolyte aqueous solutions.

Recently we systematically re-examined the issues in the quantitative and polarization analysis of the SH response from the molecular interface.[54–56] The non-resonant SHG response in different polarization combinations can be used to determine the orientational parameter of the interfacial water species. With this knowledge, the orientational and the

number density contributions to the SHG signal can be explicitly separated. Thus, the change of the interfacial thickness or depth can be quantitatively determined.

In this paper, we present the non-resonant SHG measurement on the change of the interfacial thickness or depth of the NaF, NaCl and NaBr aqueous solutions at various bulk concentrations. We found that the interfacial thickness or depth of all three solutions increased with the bulk salt concentration, following the order NaBr > NaCl ≈ NaF. These results not only confirmed the earlier observation on the increase of the interfacial thickness or depth of the NaBr and NaI aqueous solutions,[8] but also provided a quantitative measurement of the change of the thickness or depth of the NaF, NaCl and NaBr aqueous solution interfaces. Before going to the non-resonant SHG results and discussions, we shall present the theoretical background of the quantitative analysis in non-resonant SHG, and to address the issues on how the various impurities are monitored and removed from the salt samples.

II. Quantitative analysis in the non-resonant SHG

The interface selectivity of the second order nonlinear optical techniques, mainly the surface second harmonic generation (SHG) and sum frequency generation vibrational spectroscopy (SFG-VS), have been well established and demonstrated.[31,57] Quantitative analysis of the SHG and SFG-VS data has also been developed and summarized.[55,58,59] Even though the non-resonant SHG has played a key role in the early development of the surface nonlinear optical methods,[53,60,61] its lack of chemical selectivity, both electronic and vibrational, on the different interfacial species has limited its application to surface studies. However, if the SHG signal change originates from only one of the interfacial chemical species, the quantitative interpretation of the non-resonant SHG data is straightforward and can provide unique information about the interface. One recent example is the measurement and interpretation of the non-resonant SHG signal in the different polarization combinations of the neat air/water interface. It provided a strong argument for the negligible quadrupolar contribution to the interfacial SHG signal for the neat air/liquid interface.[54,55] It is therefore natural to extend it to the study of water molecules in the air/electrolyte aqueous solution interfaces.

A The general expression for the surface SHG

The SHG intensity $I(2\omega)$ reflected from the electrolyte aqueous interface is given by[56,59]

$$I(2\omega) = \frac{32\pi^3\omega^2 \sec^2\beta}{c_0^3 n_1(\omega)n_1(\omega)n_1(2\omega)}|\chi_{\text{eff}}|^2 I^2(\omega) \qquad (2.1)$$

$I(\omega)$ is the incoming laser intensity, c_0 is the speed of the light in the vacuum, β is the incident angle from the surface normal, defined as z axis in the laboratory coordinates system (x,y,z), $n_1(\omega_i)$ is the refractive index at the frequency ω_i of the medium in which the laser beam propagates. χ_{eff} is the effective macroscopic second order susceptibility. In the SHG experiment, because there is only one incident laser beam and one out-going signal beam, there are three independent polarization combinations for the χ_{eff}: namely the s-in/p-out($\chi_{\text{eff,sp}}$), the 45°-in/s-out($\chi_{\text{eff,45°s}}$) and the p-in/p-out($\chi_{\text{eff,pp}}$). Here, p denotes the polarization in the incident plane, while s the polarization perpendicular to the incident plane. With the microscopic local-field factors incorporated implicitly into the tensorial Fresnel factor L_{ii}s, the χ_{eff}s are[59]

$$\begin{aligned}
\chi_{\text{eff,sp}} &= L_{zz}(2\omega)L_{yy}^2(\omega)\sin\beta\chi_{zyy} \\
\chi_{\text{eff,45°s}} &= L_{yy}(2\omega)L_{zz}(\omega)L_{yy}(\omega)\sin\beta\chi_{yzy} \\
\chi_{\text{eff,pp}} &= L_{zz}(2\omega)L_{xx}^2(\omega)\sin\beta\cos^2\beta\chi_{zxx} \\
&\quad - 2L_{xx}(2\omega)L_{zz}(\omega)L_{xx}(\omega)\sin\beta\cos^2\beta\chi_{xzx} \\
&\quad + L_{zz}(2\omega)L_{zz}^2(\omega)\sin^3\beta\chi_{zzz}
\end{aligned} \qquad (2.2)$$

in which the χ_{ijk}s are the seven non-zero susceptibility tensors, *i.e.* χ_{zzz}, $\chi_{zxx} = \chi_{zyy}$, $\chi_{xzx} = \chi_{xxz} = \chi_{yzy} = \chi_{yyz}$ of the rotationally symmetric interface along the interface normal z, with x in the incident plane. In order to calculate the χ_{ijk} tensors in eqn (2.2) from the measured χ_{eff} values, quantitative evaluation of the effective microscopic local field factors in the interfacial layer in determination of the L_{ii} factors is essential. This issue shall be discussed in section IIC and later.

In the SHG measurement, polarization is usually fixed at either p or s, while the polarization angle Θ of the incident laser beam is varied for the full 360° using a half waveplate. Then, one has[54,55,62]

$$\begin{aligned}
I_{\text{p}} &\propto |\chi_{\text{eff,p}}|^2 = |\chi_{\text{eff,pp}}\cos^2\Theta + \chi_{\text{eff,sp}}\sin^2\Theta|^2 \\
I_{\text{s}} &\propto |\chi_{\text{eff,s}}|^2 = |\chi_{\text{eff,45°s}}\sin 2\Theta|^2
\end{aligned} \qquad (2.3)$$

In the case of non-resonant SHG, each of the $\chi_{\text{eff,pp}}$, $\chi_{\text{eff,sp}}$ and $\chi_{\text{eff,45°s}}$ terms is real, and their relative value can be obtained from fitting the experimental data with eqn (2.3) by knowing the relative signs between them. The relative signs can be determined with the measurement of the SH signal in the 45° polarization as described previously.[55]

B Origins of the non-resonant SHG signal from the electrolyte solution interface

There are water molecules and possibly ions in the interfacial region of the air/electrolyte aqueous solution. Therefore, the non-resonant SHG signal can come from the contributions of the water species, the ionic species and also from the interfacial-potential-induced SHG due to the possibly non-uniform distribution of the ionic species in the interfacial region. The last term is through the mechanism of electric-field-induced second harmonic generation (EFISHG).[63–65] Therefore,

$$\chi_{\text{eff}}^{\text{total}} = \chi_{\text{water}}^{(2)} + \chi_{\text{ions}}^{(2)} + \chi_{\text{water}}^{(3)}\Phi(0) \qquad (2.4)$$

where $\Phi(0)$ is the surface potential at the plane of the interface where the net charges reside. In cases when the bulk electrolyte (1 : 1 charge) concentration is less than 2 M, $\Phi(0)$ can be calculated with the so-called Gouy–Chapman model for the

electric double layer (in SI units),[22,66,67]

$$\Phi(0) = \frac{2kT}{ze}\sinh^{-1}\left(\sigma\sqrt{\frac{1}{8\varepsilon\varepsilon_0 kTC}}\right) \quad (2.5)$$

where C is the bulk electrolyte concentration, k is the Boltzmann constant, T is the temperature of the solution, z is the charge number of the unit ion, σ is the charge density in the plane of interface, ε is the dielectric constant of the bulk solution, and ε_0 is the permittivity of the vacuum.

The EFISHG term in eqn (2.4) is the contribution from the polarized water molecules in the vicinity of the interfacial region induced by the interfacial electric field generated from the net charge at the plane of the interface. This term is generally negligible in the case of resonant SHG, where the $\chi^{(2)}$ terms from the interfacial chemical species are generally more than one order of magnitude bigger than the EFISHG term.[63–65]

Here the EFISHG term in eqn (2.4) is invoked because recent MD simulations predicted that the larger and more polarizable anions, such as Br^- and I^- anions, are enriched at the interface and the cations are separated in the layer below to form an electric double layer.[4,15] We shall show that the EFISHG term in the non-resonant SHG from the simple electrolyte aqueous solution interface is actually negligible, indicating a very weak electric double layer structure at such interfaces.

The second term in eqn (2.4) is also negligible in the non-resonant SHG. Although the linear polarizability of the anions, like Cl^- and Br^-, may have larger values than that of the water molecule,[68] the second order hyperpolarizability of these ions is essentially zero because the ions are centrosymmetric particles.[69] The hyper-Rayleigh scattering signal at 400 nm from the 5.0 M NaBr aqueous solution was measured in our laboratory. It is just the same as that of the neat liquid water. This indicates that the second order hyperpolarizability of the ions are generally negligible in comparison with that of the water molecules. In addition, because the second term in eqn (2.4) is negligible, no change of the SHG signal from that of the neat air/water interface was observed in our experiment for the interface of the relatively low electrolyte concentration (10^{-3} M) aqueous solutions. While in the case of the resonant SHG, the Jones–Ray effect at such low electrolyte concentration was reported by Saykally *et al.* for some inorganic salt solution interfaces.[33,37]

Therefore, in the non-resonant SHG measurement of the simple inorganic electrolyte aqueous solution interface, only the first term in eqn (2.4) dominates. This fact greatly simplified the analysis in this study.

C Quantitative analysis of the SHG signal from the interfacial water molecules

Quantitative analysis of the non-resonant SHG from the interfacial water molecules was studied in detail in one of our recent studies on the neat air/water interface.[54,55] In order to apply it to the electrolyte solution interfaces, one has to assume that the second order hyperpolarizability, *i.e.* the β_{ijk} tensor elements, of the water molecules does not change under the influence of the ions. Quantum calculation of the second order hyperpolarizability of the water molecule in a strong electric field from 10^5 to 10^7 V cm^{-1} showed that it varied insignificantly from the values of the free water molecule.[70] This suggests that, indeed, the β_{ijk} tensor elements of the water molecule can be considered unchanged with the presence of the ions.

For molecules with C_{2v} symmetry, there are seven nonzero microscopic polarizability tensor elements $\beta_{ijk}(i,j,k = a,b,c)$ in molecular coordinates system (a,b,c): namely, β_{ccc}, β_{caa}, β_{cbb}, β_{aca}, β_{aac}, β_{bcb} and β_{bbc}, with $\beta_{aca} = \beta_{aac}$ and $\beta_{bcb} = \beta_{bbc}$ for the SHG process. When the optical frequency is far below the resonance, β_{ccc} is usually negligible. By defining $R = (\beta_{caa} + \beta_{cbb})/(\beta_{aca} + \beta_{bcb})$, one has,[54,55]

$$\frac{\chi_{zxx}}{\chi_{xzx}} = \frac{(R-2)D + (R+2)}{-RD + (R+2)}$$
$$\frac{\chi_{zzz}}{\chi_{xzx}} = \frac{2(R+2)D - 2(R+2)}{-RD + (R+2)} \quad (2.6)$$

Here $D = \langle\cos\theta\rangle/\langle\cos^3\theta\rangle$ is the orientational parameter with θ as the tilt angle of the water dipole axis from the interface normal, $\langle\ \rangle$ denotes the ensemble average over the whole orientational distribution. After quantitative evaluation of the effective microscopic local field factors in the interface layer as discussed later, the two ratios χ_{zxx}/χ_{xzx} and χ_{zzz}/χ_{xzx} can be accurately obtained from the polarization SHG measurement as described in section IIA. Then the R and D values can be readily obtained with good accuracy, using eqn (2.6).[54,55]

Now with the orientational parameter D known, the relative number of water molecules contributing to the measured SHG signal from the interface of the different electrolytes as well as different electrolyte concentrations can be calculated from the changes of the corresponding SHG intensities. Simply stated,

$$I_{2\omega} \propto |\chi_{\text{eff}}|^2 \propto N_s^2|r(\theta)|^2 \quad (2.7)$$

Here N_s is the interface number density of the water molecule and $r(\theta)$ is the orientational function directly related to the orientational parameter D.[55,56]

III. Experimental

A Experimental setup

The SHG experimental setup is as in the previous reports.[54,56] A broadband tunable mode-locked femtosecond Ti:sapphire laser (Tsunami 3960C, Spectra-Physics) is used for the reflected-geometry SHG measurement. Its high-repetition rate (82 MHz) and short pulse width (80 fs) make it suitable for detection of the weak second-harmonic signals. The long term power and pulse-width stability also make it easy for quantitative analysis of the SHG data.[71] One only needs to check whether the SHG signal from the neat air/water interface changed before, during and after the day's experiment. Our experiences were that, in a temperature controlled environment, such a signal varied normally within 3% in the day-to-day operations with the same laser setting and the same optical setup. Therefore, no special normalization procedure was required. The 800 nm fundamental laser beam is focused on the solution interface at the incident angle of $\beta = 70°$, and the

SHG signal at 400 nm is detected with a high-gain photomultiplier tube for single photon counting (R585, Hamamatsu) and a photon counter (SR400, Stanford Research Systems). Typically the dark noise level is less than 1 count s^{-1}, better than reported previously.[54] The typical laser power is 500 mW. The efficiency of the detection system for the p polarization is 1.23 times of that for the s polarization. A cylindrical Teflon beaker (ϕ 50 × 6 mm) is used to host the solution. The optical polarization control and the SHG data acquisition are programmed and collected with a PC. It takes about 150–300s to collect the polarization curve. The room temperature is controlled at 22.0 ± 1.0 °C, and the humidity in the room is controlled around 40%.

B Chemicals

In the experiments, the liquid water was purified with a Millipore Simplicity 185 (18.2 MΩ cm) from double distilled water. The salts used were purchased from the ACROS (ACS reagent grade, 99% + purity). Before the preparation of the salt solution, the salts were baked at around 500 °C for more than 6 hours in order to remove the organic impurities, a practice now adopted by different groups.[47] The glassware was cleaned with hot chromic acid and then rinsed several times with Millipore water. The SFG spectra of the solution surfaces were checked in the 2800 to 3000 cm^{-1} range to ensure that there was no organic contamination. SHG fluctuation measurement was used to check whether the solution interface was contaminated with the floating microparticles, possibly from the carbonized organic contaminants in the salt, which cannot be detected with the SFG measurement. Such carbonaceous particles can be removed from the solution by filtering through a syringe with a 0.22 μm membrane filter made of PVDF material by Millipore (Durapore GVWP01300). Cross-checking with the SFG spectra and the SHG fluctuation measurement is crucial to ensure a clean surface. The details are discussed below.

C Monitoring and removal of the trace organic and microparticle contaminants

Two kinds of trace contaminants can affect the non-resonant SHG measurement of the electrolyte solution interfaces. They can be identified with the SFG-VS and SHG fluctuation measurement. The first is the trace organic contaminants in the salt sample. The second is the microparticles floating at the solution interface. Organic contaminants can adsorb onto the solution interface. Using SFG-VS to monitor the C–H stretching vibrational region can help determine most of the possible organic contaminants. SHG fluctuation measurement can detect the microparticles floating on the solution surface.

Fig. 1 is the SFG spectra in the ssp polarization combination of the interface of the neat air/water interface, the 3.0 M NaBr aqueous solution with and without baking the NaBr salt before making the solution. The experimental detail was described elsewhere.[50,72] The SFG spectral peaks for the unbaked NaBr salt solution around 2850 cm^{-1}, 2880 cm^{-1} and the broad band around 2920–2950 cm^{-1} are clearly the $-CH_2$ and $-CH_3$ stretching vibrational mode and their Fermi resonance peaks, respectively.[58,72,73] The intensity of

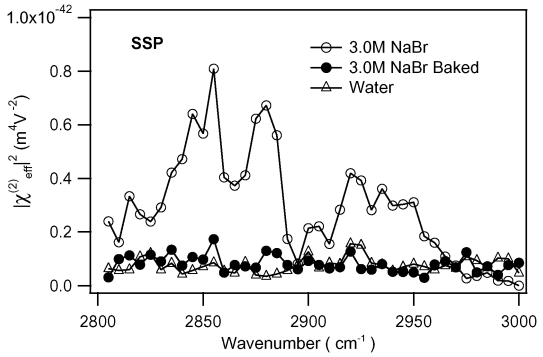

Fig. 1 The ssp SFG spectra of the surfaces of the neat water (△), the 3.0 M sodium bromide solution (○) and the 3.0 M baked sodium bromide solution (●) in the 2800 to 3000 cm^{-1} region. The incident angles in the SFG experiment are: Vis = 63°, IR = 55°.

the 2880 cm^{-1} peak is about one-tenth of that for the neat air/methanol interface,[74] indicating a surface coverage of the $-CH_3$ group of the organic contaminate molecules in the range of 0.1 to 0.3, which cannot be ignored in any of the measurement. Generally the higher the unbaked salt concentration, the higher the SFG spectra intensity. The SFG spectra of the baked sample surface in Fig. 1 indicates that the organic contaminants were efficiently removed. Further tests showed that the NaCl, NaBr and NaI samples from the ACROS all had some trace organic contaminants, and the baking procedure can efficiently remove them as monitored by the SFG spectra. However, for the NaF sample from the ACROS, no such measurable organic contaminant was found.

Allen *et al.* used activated carbon to remove the organic contaminants from the salt solution,[8] and recently they reported using the baking method.[47] They also used the SFG-VS to monitor the removal of the organic contaminants. In the past experimental studies, some groups used the salt samples as received.

The SFG spectra cannot tell whether there are microparticles at the solution interface. Microparticles can generally exist in the solutions with or without baking the salt. We discovered this through fluctuation measurements of the solution interface using non-resonant SHG. The fluctuation of the SHG signal indicates that the interface is heterogeneous in nature.[75] In SHG measurement, the laser beam is focused down to about 30 μm, so the diffusion of the sub-micron sized small particles at the solution interface can be observed. Since the focal spot in the SFG measurement is generally much larger (generally up to several hundred micrometers), such a fluctuation has not been observed in SFG measurements. On the other hand, the microparticles may not have a spectral response which the SFG-VS can detect. Therefore, the SHG fluctuation measurement is a unique tool to monitor them.

Fig. 2 shows the non-resonant SHG measurement in the pp polarization combination over a period of 600 seconds of the interface of a 0.1 M NaBr and 1.0 M NaCl solution with or without syringe filtration. It is surprising that some spikes are four times that of the SHG signal from the surface free of such particles (see the middle panel in Fig. 2). After filtration, all the spikes disappeared completely as shown in the bottom panel in Fig. 2. The SHG signal fluctuation of the unfiltered sample

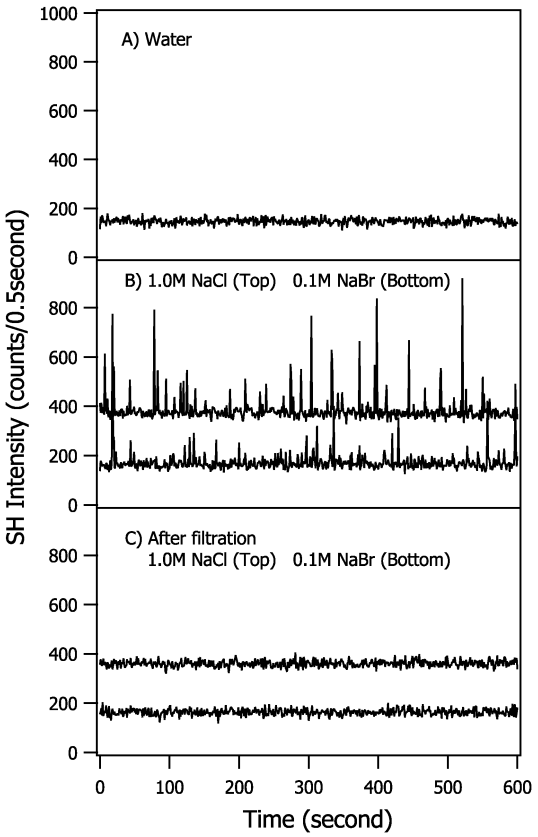

Fig. 2 The SHG (400 nm) fluctuation measurements (p-in/p-out polarization combination): (A) neat water, (B) 1.0 M NaCl and 0.1 M NaBr without filtration, and (C) 1.0 M NaCl and 0.1 M NaBr after filtration. The SHG signal from the NaCl solution was offset for clarity.

solution as shown in Fig. 2 can make the SHG measurement subject to significant errors. Generally, the higher the salt concentration, the larger the magnitude of the fluctuation. We found that the NaCl, NaBr and NaI samples from the ACROS all exhibited such SHG signal fluctuations, and all spikes can be removed after the filtration. On the other hand, the NaF samples of different batches from the ACROS generally did not show such fluctuation with or without filtration.

Because the organic contaminants and the microparticles were found in the same sample, it is reasonable to surmise that either there were microparticles in those salts originally, or the microparticles were formed in the baking process. Baking the salt may carbonize the organic contaminants to form carbonaceous microparticles. There was no SHG fluctuation over a period of several hours ever being observed from the neat air/water interface in our laboratory. This ensured that the laboratory environment was free of such particles.

The NaI data is not included in this report because after baking and filtration, the SHG signal from the NaI solution surface is free of fluctuation, but the SHG signal cannot be stabilized in the open environment even in the dark room. It is known that NaI is light sensitive.[9] Therefore, we suspect that there were other unknown causes for such instability of the NaI samples.

The pure salt samples with the same purity grade label from the Sigma-Aldrich also showed the same behavior as those from the ACROS when monitored with the SFG spectral and SHG fluctuation measurement.

In summary, baking and filtration are effective measures to remove the organic contaminants and microparticles from inorganic salt solutions, respectively. The organic contaminants or micro-particles can be monitored with SFG spectra or with the SHG fluctuation measurement, respectively. With these precautions, the non-resonant SHG measurement results in this report were reproducible with a high accuracy, which ensured the quantitative analysis as presented below.

IV. Results and discussions

A The polarization dependent non-resonant SHG results

To our knowledge, the non-resonant SHG signal from the neat air/water interface is one of the weakest among all the interfaces. However, the sensitivity of the non-resonant SHG detection of the weak signal from the air/water interface using the high-repetition laser pulses plus the single photon counting electronics has been achieved since the early era of SHG studies.[64,76] With the development of the high-repetition rate femtosecond lasers, the detection sensitivity has been improved by about two to three orders of magnitude.[54,65] Recently it was shown that by making the p and s polarization measurements while changing the polarization of the incoming laser field by a full 360°, the strong and weak components of the three independent polarizations can be accurately determined.[54,55] This is essential for the polarization analysis as illuminated with eqn (2.6).

Fig. 3 shows the p and s polarization detection of the non-resonant SHG from the 3.0 M NaBr solution interface. Their polarization angle dependence is the same as that of the neat air/water interface. In addition, the polarization angle dependence for the 45° detection also follows the same pattern as that for the neat air/water interface. This latter fact indicated that the $\chi_{eff,pp}$, $\chi_{eff,sp}$ and $\chi_{eff,45°s}$ terms in eqn (2.3) all have the same sign.[55] Therefore, the p and s detection curves can be used to uniquely determine their magnitudes using eqn (2.3).

As in Fig. 3, the I_{pp} is about 390 counts per second, the $I_{45°s}$ is about 135 counts per second, while the I_{sp} is less than 15 counts per second. Therefore, direct measurement of the small I_{sp} signal is subject to much larger statistical errors.[76–79] This would influence the accuracy in the polarization analysis. As discussed previously,[54,55] fitting the p and s curves in the full 360° can provide accurate and reproducible values for the smaller components, *i.e.* the I_{sp} or the $\chi_{eff,sp}$, which is more than a order of magnitude weaker than the I_{pp} and $I_{45°s}$ intensities. This procedure of data collection and analysis is essential in this study because even though the difference of the non-resonant SHG intensity as well as the change of its polarization dependence for different bulk concentrations are generally small, small changes can still be quantitatively measured, such as for the NaF and NaCl solutions, whose electrolyte concentration dependence were generally hard to be established in other studies.

For the NaF, NaCl and NaBr solutions in different concentrations, the p, s and 45° curves followed the same pattern as the neat air/water interface. The I_{pp}, I_{sp}, and $I_{45°s}$ SH

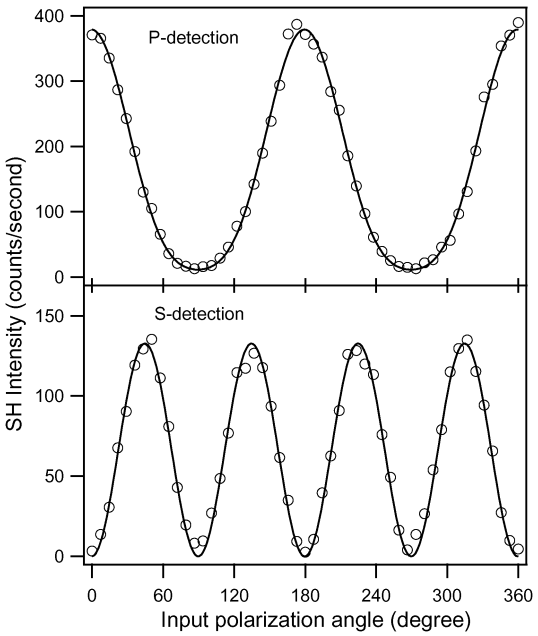

Fig. 3 Polarization SHG (400 nm) measurement results of 3.0 M NaBr solution interface in the *p* detection (top panel) and the s detection (bottom panel). The lines are the fitting curves using eqn (2.3). The correction factor for the s detection data is 1.23.

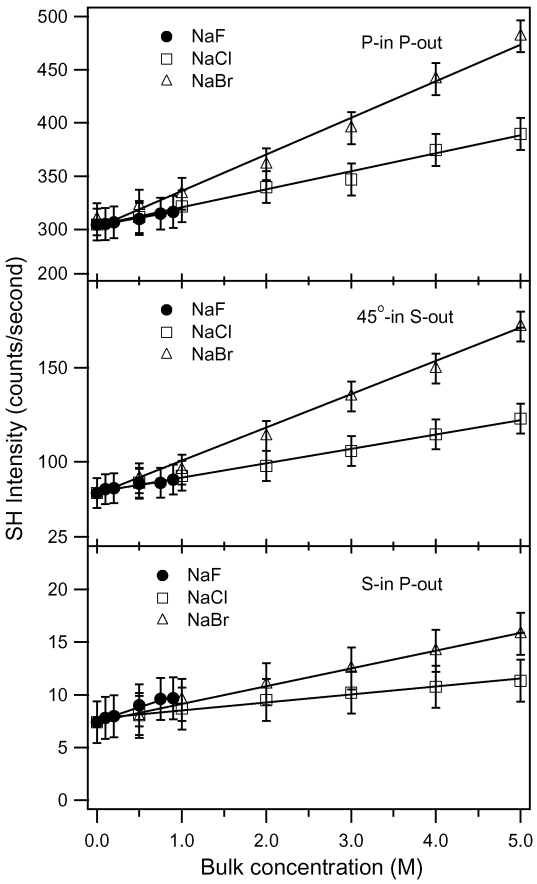

Fig. 4 Polarization and concentration dependent SHG (400 nm) data for the NaF, NaCl and NaBr solution interfaces, obtained by fitting the s and p detection data measured for each concentration and each salt solution. There is a correction factor of 1.23 for the 45°-in/s-out data.

intensities thus obtained for the different samples are plotted in Fig. 4. The NaCl and NaBr concentrations are up to 5.0 M, while the NaF concentration is only up to 0.9 M. This is because the saturation concentration of NaF at the ambient temperature is only 0.98 M (4.13 g NaF per 100 g water), while the NaCl is 6.2 M (36.0 g NaCl per 100 g water) and NaBr is 9.2 M (94.6 g NaBr per 100 g water).[80]

According to Fig. 4, the SHG signal increases monotonically with the bulk electrolyte concentration for the three salts in the different polarization combinations. Furthermore, the NaBr lines in all three polarization combinations have the bigger slope, with the only exception of the I_{sp} of the NaF.

These data clearly show that all the three salts enhanced the non-resonant SHG from the electrolyte aqueous solution interface as the bulk concentration increases. However, in the MD simulations and the SFG-VS measurements by Allen *et al.*, only the NaBr and NaI showed a significant presence at the interfacial region of the aqueous solution.[3,4,8] In comparison, Richmond *et al.* reported that the interfacial hydrogen bonding structure was affected by NaF.[9] Nevertheless, the general trend in the SHG data reported here is consistent with the MD simulation results and the SFG-VS measurements in that the larger and more polarizable anions have the bigger effect on the water molecules at the aqueous interface.

B The increased interfacial thickness of the water molecules

As discussed previously,[54] the contribution to the non-resonant SHG signal from the air/water interface is from the hydrogen bonded water molecules below the topmost layer, because the dipole vector of the water molecules at the topmost layer lies almost parallel to the plane of interface,[50,51,81–91] and their contribution to the measured non-resonant SHG has to be negligible. The SFG-VS measurements showed that the narrow free O–H spectral peak around 3700 cm^{-1} in the ssp polarization, which belongs to the water molecules in the topmost interfacial layer, remained almost unperturbed with the addition of the salts.[3,8,9] Therefore, the increase of the SHG signal with the increase of the bulk salt contribution is from the water molecules other than the topmost layer water molecules. This indicates that the calculation according to eqn (2.6) should be valid as discussed previously for the neat air/water interface.[54]

Table 1 listed the calculated results of the χ_{zxx}/χ_{xzx} and χ_{zzz}/χ_{xzx} ratios for all samples using eqn (2.2) and eqn (2.3). The values of the water susceptibility ratio R and the orientational parameter D of the interfacial water molecules according to eqn (2.6) are also listed. Accordingly, the apparent orientational angle θ is calculated from the D values assuming a δ orientational distribution. As in the previous report on the neat air/water interface,[54] the interfacial refractive index used in the calculation followed the model proposed by Zhuang *et al.*[59]

The R value as defined as the $(\beta_{caa} + \beta_{cbb})/(\beta_{aca} + \beta_{bcb})$ ratio is the property of the hydrogen bonded water molecule. Therefore, it is not surprising that the R values in Table 1 are all the same as that for the neat air/water interface, even though the SHG intensities for the different samples were

Table 1 The results for the χ_{zxx}/χ_{xzx}, χ_{zzz}/χ_{xzx}, R, D and θ (assuming δ distribution) for the neat water, NaF, NaCl and NaBr salt solution interfaces

NaX	Concentration/M	χ_{zxx}/χ_{xzx}	χ_{zzz}/χ_{xzx}	R	D	θ
Water	0.0	0.27 ± 0.03	2.54 ± 0.06	0.68 ± 0.02	1.72 ± 0.02	40.3 ± 0.4
NaF	0.1	0.27 ± 0.03	2.52 ± 0.06	0.68 ± 0.02	1.71 ± 0.02	40.1 ± 0.4
	0.2	0.28 ± 0.03	2.52 ± 0.06	0.68 ± 0.02	1.71 ± 0.02	40.1 ± 0.4
	0.5	0.29 ± 0.03	2.50 ± 0.06	0.68 ± 0.02	1.71 ± 0.02	40.1 ± 0.4
	0.75	0.30 ± 0.03	2.51 ± 0.06	0.69 ± 0.02	1.71 ± 0.02	40.1 ± 0.4
	0.9	0.30 ± 0.03	2.50 ± 0.06	0.69 ± 0.02	1.70 ± 0.02	39.9 ± 0.4
NaCl	0.5	0.27 ± 0.03	2.51 ± 0.06	0.68 ± 0.02	1.71 ± 0.02	40.1 ± 0.4
	1.0	0.28 ± 0.03	2.53 ± 0.06	0.68 ± 0.02	1.71 ± 0.02	40.1 ± 0.4
	2.0	0.28 ± 0.03	2.50 ± 0.06	0.68 ± 0.02	1.71 ± 0.02	40.1 ± 0.4
	3.0	0.28 ± 0.03	2.45 ± 0.06	0.68 ± 0.02	1.70 ± 0.02	39.9 ± 0.4
	4.0	0.28 ± 0.03	2.45 ± 0.06	0.68 ± 0.02	1.70 ± 0.02	39.9 ± 0.4
	5.0	0.27 ± 0.03	2.43 ± 0.06	0.67 ± 0.02	1.70 ± 0.02	39.9 ± 0.4
NaBr	0.5	0.27 ± 0.03	2.51 ± 0.06	0.67 ± 0.02	1.71 ± 0.02	40.1 ± 0.4
	1.0	0.28 ± 0.03	2.48 ± 0.06	0.68 ± 0.02	1.70 ± 0.02	39.9 ± 0.4
	2.0	0.28 ± 0.03	2.42 ± 0.06	0.67 ± 0.02	1.69 ± 0.02	39.7 ± 0.4
	3.0	0.28 ± 0.03	2.37 ± 0.06	0.67 ± 0.02	1.68 ± 0.02	39.5 ± 0.4
	4.0	0.28 ± 0.03	2.37 ± 0.06	0.67 ± 0.02	1.68 ± 0.02	39.5 ± 0.4
	5.0	0.27 ± 0.03	2.34 ± 0.06	0.67 ± 0.02	1.68 ± 0.02	39.5 ± 0.4

different. Furthermore, this value is in good agreement with the calculated value according to the Franken and Ward's treatment of the R value using the dispersion relationship.[54,92] Here, $R \neq 1$ indicates that the so-called Kleinman symmetry generally fails for the water molecule even though the SHG wavelength is far from that of the electronic resonance.[54,92,93]

Furthermore, the invariance of the R values as listed in Table 1 provides a solid confirmation for the assumptions as made in the section IIB about the origin of the SHG signal. The assumption is that the non-resonant SHG signal is dominated by the contributions from the interfacial water molecules only, without the contribution from the EFISHG terms and the interfacial $\chi^{(2)}_{\text{ion}}$ term in eqn (2.4). If these two terms are not negligible, the invariance of the R value as obtained here is not possible.

The D and θ values, as compiled in Table 1 and as plotted in Fig. 5, only exhibited slight changes with the different samples. To be precise, the D values for the NaBr solutions had a slightly larger change with the bulk concentration than those of the NaF and NaCl. However, even for NaBr, the change is small when the concentration is as high as 5.0 M. As the orientation remained almost unchanged, the significant increase of the observed SHG signal has to be the result of the increasing number density of the interfacial water molecules. Assuming the interfacial area density of the water molecules is the same, the increase of the interfacial number density must be proportional to the increase of the interfacial thickness or depth of the interfacial water layer.

Here, because the calculation of the R and D values according to eqn (2.6) depends on the choice of the effective refractive index or the effective microscopic local field factors of the interfacial layer,[59] the issue on whether the addition of salt into the bulk water may significantly alter these factors needs to be addressed. The treatment of the effective refractive index of the interfacial layer based on the modified Lorentz model by Zhuang *et al.* may not be suitable for the closely packed Langmuir monolayers with chromophores of strong linear polarizability.[58,94–96] However, this model has been shown to be quite accurate for the interfaces of the simple

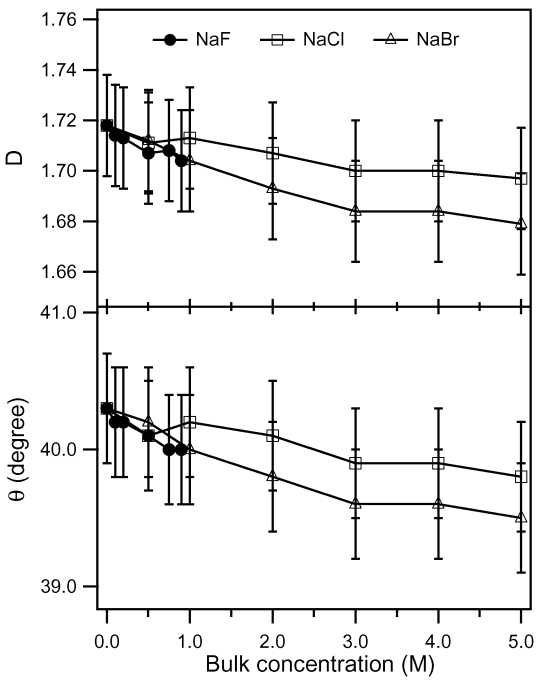

Fig. 5 The orientational parameters D (top panel) and the apparent orientational angles θ (bottom panel) for the NaF, NaCl and NaBr solution interfaces with different bulk concentrations.

liquids and pure liquid water.[48,50,54,58] Fordyce *et al.* showed that for the neat air/water interface, the temperature dependent local field correction only caused a small variation in calculating the χ_{ijk} tensor values.[77] It is known that, at room temperature, the refractive index of the aqueous solution at high salt concentration increases by only 0.04 for a 5 M NaCl solution from that of the neat liquid water.[97] If there is a increase of the effective refractive index of the salt aqueous solution interfacial layer, it should also be the same magnitude or less. According to the modified Lorentz model by Zhuang *et al.*, it is about half of the change for the bulk aqueous solution. Our calculation, with or without such changes, for

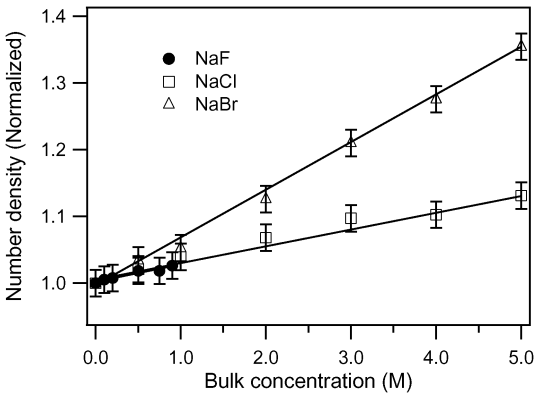

Fig. 6 The relative interfacial density of the water molecules at the NaF, NaCl and NaBr salt solutions with different bulk concentrations.

the effective refractive index of the interfacial layer for various high salt concentrations showed that the variation of both the R and D values is less than 0.02. Therefore, the effect of the changing effective refractive index of the interfacial layer at various bulk salt concentrations on the R and D values is indeed negligible.

Now, using the relationship in eqn (2.7) and the SHG data in different polarizations, the relative number density at the interfacial region contributing to the non-resonant SHG signal is calculated and plotted in Fig. 6. The interfacial thickness or depth for the NaBr aqueous solution increased almost linearly by about 30% as the NaBr bulk concentration increased from 0 to 5.0 M; for NaCl solutions, it increased by about 10% as the concentration increased from 0 to 5.0 M; while for NaF, about a 3% increase of the interfacial thickness or depth as the bulk concentration went to 0.9 M. It is not yet clear whether the NaF or the NaCl has a bigger effect on the interfacial thickness at the same bulk concentration.

In the SFG-VS study by Allen *et al.*,[8] the increase of the interfacial depth was reported for NaBr and NaI solutions, but not for the NaF and NaCl solutions. In contrast, the non-resonant SHG data here show that not only did the NaBr increase the interfacial thickness, but the NaF and NaCl (to a lesser extent) also did the same. Therefore, the specific anion effects on the interfacial water structure are not limited to the larger and more polarizable anions, such as the Br^- and the I^- anions.

Further comparison of the SHG and the SFG results raises more questions. The SHG results here shows increase of the interfacial thickness for all three salts. But in the SFG results, the intensity of the hydrogen bond spectra decreased some for the NaF, and increased some for the NaBr, with almost little change for the NaCl.[9] One can speculate that this might be due to the fact that while SHG probes the second order electronic polarizability of the water molecule in the interfacial region, the SFG-VS also probes the second order vibrational or infrared polarizability. The latter might be more sensitive to perturbation by anions in the nearby environment. This can also explain the fact that in the SFG spectra, the intensity of the 3400 cm^{-1} band changed differently from that of the 3200 cm^{-1} band. SFG vibrational spectra are certainly sensitive to these two kinds of hydrogen-bonded water species, while the non-resonant SHG simply cannot tell the difference between them. This is also supported by the invariance of the R value for the interfacial water molecules as obtained above. Therefore, the non-resonant SHG is a better tool to characterize the interfacial thickness or the depth, while the SFG spectra is better to probe the detail changes of the interfacial hydrogen bonding structure.

One often wonders to what depth the interface selective SHG and SFG techniques are probing. The sensitivity of the observed increase of the interfacial water depth suggests that it is indeed only the interfacial layer that is probed. If the non-resonant SHG were already probing the average of the many layers of the water molecules into the bulk beyond the interfacial layer, there should not have been such a sensitivity to the increase of the interfacial water depth when the salt is added into the aqueous solution. On the other hand, a more than 30% increase of the interfacial water depth at higher NaBr concentration is so significant that it also excludes significant bulk water contribution to the observed non-resonant SHG signal.

C The orientational order of the interfacial water molecules

It is known that both the MD simulations and the sum frequency spectra are difficult to compare with density and orientation profiles at the air/water interface.[8,9] Here, with the orientational parameter quite accurately determined from the polarization SHG measurements, the specific ion effect on the orientational order of the interfacial water molecules can be discussed.

According to Simpson and Rowlen,[98] when the apparent orientational angle θ value is close to the so-called "magic angle" of 39.2°, it is impossible to know the actual orientation and its distribution of the interfacial water molecules. Therefore, the small change of the D and θ values around 40°, as compiled in Table 1 and plotted in Fig. 5, cannot be used to rule out the possibility that the interfacial water molecules are significantly more disordered as more salt is added. However, it is highly unlikely that the interfacial water molecules became more disordered with the addition of salts, from the SHG intensity data.

Firstly, if the addition of more salts into the liquid water caused disorder of the water molecules, the interface itself would become more close to the disordered bulk liquid, or in other words, the interface would become thinner. Therefore, the total SHG signal should have decreased, if one still believes that the surface nonlinear spectroscopy is intrinsically the measurement of the order or the anisotropy of the interface.

Secondly, it is hard to comprehend the picture that while the interfacial water molecules were becoming more disordered as more salt was added, and in the meantime there were more water molecules in the interfacial region that started to contribute to the SHG signal. These two completely opposite trends are not likely to happen simultaneously.

Orientationally-sensitive and orientationally-insensitive measurement with the polarization dependent SHG were discussed by Simpson and Rowlen,[99,100] and further discussed by Rao *et al.*[55,56,58] In general, SHG or SFG measurement in different polarization combinations should have different

sensitivity to the changing molecular orientation and orientational distribution. Because of this different sensitivity to the orientational order, polarization measurement in SHG can provide accurate measurement on the orientational order of the interfacial molecular ensemble.

In Fig. 4, the slope of the I_{pp} against the bulk salt concentration is slightly smaller than that for the I_{sp} and the $I_{45°s}$ for the three salts. This means that the $I_{pp}/I_{45°s}$ ratio becomes smaller as the bulk concentration increases. According to eqn (2.7), this means that the ratio $|r_{pp}(\theta)|^2/|r_{45°s}(\theta)|^2$, which is purely dependent on the orientation profile of the interfacial water molecules and is independent from the surface water number density, changes accordingly with the bulk salt concentration. This change is evident even though the calculated D values in Table 1 changed only by −0.04 for the 5.0 M NaBr solutions from that of the neat air/water interface. This change is small but is twice the value of the statistical error. Therefore, the change of the orientational order of the interfacial water molecule is by all means real.

In most cases, the smaller $D = \langle\cos\theta\rangle/\langle\cos^3\theta\rangle$ value represents a better orientational order, especially for the Langmuir monolayer where the surface number density of the molecules are known.[56] However, according to Simpson and Rowlen,[56,58,98] the dependence of the D value on the orientational angle and its distribution profile is not simple. D is certainly a better description of the orientational order than the orientational angle θ, because D is calculated from the experimental measurement directly without any assumption of the orientational distribution profile. Since the salt effects on the D value of the interfacial water molecules is so small, it is safe to conclude that the orientational order of the water molecules at these interfaces remained almost unchanged, while the interfacial thickness increased evidently from that of the neat air/water interface.

D The weak electric double layer at the salt solution interface

The recent MD simulations concluded that an electric double layer with a net negative charge can be formed at the interface of the electrolyte aqueous solution because of the simulated significant enhancement of the anion adsorption at the air/water interface, especially for the larger and more polarizable anions.[4,15,18] For example, the 1.2 M NaBr solution would have a 2.10 × 1.2 M Br^- anion concentration at the Gibbs dividing surface at the air/water interface, while the counterion concentration is 0.81 × 1.2 M Na^+ at the same Gibbs dividing surface. The net negative charge density is about 105 $Å^2$ at this interface and it can create a surface potential of −0.051 V, according to the Gouy–Chapman model of the electric double layer at the charged interface. This interfacial potential would further polarize the water molecules in the bulk, and result in a significant contribution to the SHG signal through the so-called electric-field-induced SHG (EFISHG) mechanism.

The EFISHG from the net charge at the air/water and silica/water interface was well characterized by Eisenthal *et al.* in the early 1990s.[63,64] According to those studies, the EFISHG from the polarized water molecules in the vicinity of the air/water interface by the net negative charge at the air/water interface would decrease the SHG signal from that of the neat air/water interface. This is to say that the total SHG signal from the negatively charged NaBr aqueous solution interface would be smaller than that of the neat air/water interface if the interfacial layer thickness for the 1.2 M NaBr solution remains the same as that of the neat air/water interface. This is directly opposite the observed trend that the SHG signal increased significantly with the NaBr bulk concentration.

In order to further elaborate this, some quantitative calculations of the EFISHG term need to be presented here. This can be easily done with the parameters from the literature.[64] Accordingly, when the SHG intensity for the neat air/water interface is used to normalize all the terms in eqn (2.4), *i.e.* let $\chi^{(2)}_{water} = 1$, then $\chi^{(3)}_{water} = 4.0$. Thus, if we assume $\chi^{(2)}_{ion}$ is negligible and the interfacial thickness remains the same, then $\chi^{total}_{eff} = 0.80$, and the total SHG signal shall be $0.80^2 = 0.64$ of that for the neat air/water interface. It is an astonishing 36% drop!

If one assumes that the total net charge at the NaBr solution interface will be proportional to that of the 1.2 M solution for other concentrations, then the interface Br^- anion concentration is 2.1–0.81 = 1.29 times of the bulk concentration. Converting this into the two dimensional surface charge density and using the Gouy–Chapman model (eqn (2.5)) in eqn (2.4), the calculated total SHG intensity is then shown as the bottom curve in Fig. 7. In the simulation, the adsorption saturation effect at high electrolyte concentration was not considered as in the literature,[101] since the lower concentration part of the curve has the most dramatic change of the surface potential. On this curve, even when the NaBr bulk concentration is less than 0.1 M, the small amount of the net negative charge at the interface can cause a significant drop of the SHG signal because the charge screening length is long at such a low bulk ionic concentration. Such an effect not only cannot be correlated to the observed SHG data as in Fig. 4, but also it is clear that they simply went into the opposite directions. This suggests that the EFISHG contribution is simply not in the observed SHG data, so as the strong net negative charge at the interface as predicted from the MD simulations.

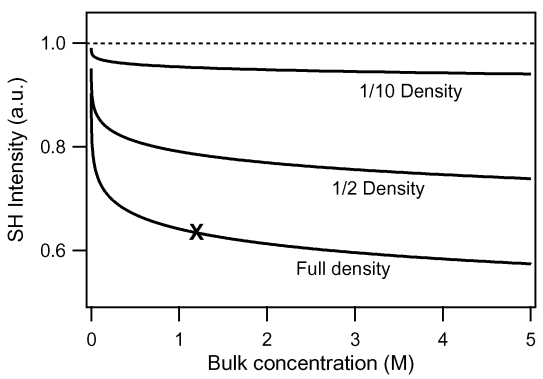

Fig. 7 Simulated SHG signal with the EFISHG contribution for the NaBr solution interface with the enriched Br^- adsorption as predicted by the MD simulation.[4,15,18] X marks the result for the 1.2 M NaBr bulk concentration. Also presented are the EFISHG simulation results for the 1/2 and the 1/10 of the surface anion enrichment of the MD simulation results. The drop of the SHG intensity with the bulk concentration is an opposite trend to the SHG data in Fig. 4.

In the section IVB, the invariance of the R value for all three salt solutions in different concentrations without considering the contribution from the EFISHG term also suggests that the EFISHG effect has to be negligible. The Fig. 7 also presents the simulated SHG curve with the EFISHG term for the much lower surface negative charge excess, namely 1/2 and 1/10 of the net charge density. Even the 1/10 charge density curve shows a noticeable decrease of the SHG signal. Therefore, the net negative charge density at the NaBr aqueous solution interface has to be even smaller.

Recently, Cremer's group probed the specific anion adsorption to a neutral macromolecule interface with electric-field-induced SFG vibrational spectroscopy of the interfacial water molecules.[101] They pointed out that the water SFG spectral peak induced by I^- at the air/macromolecule/aqueous interface is about 100 times stronger than that at the air/water interface. In their Gouy–Chapman–Stern simulation, the maximum surface charge density is 50 $Å^2$ per charge. Using the same model, one can also conclude that the preferable adsorption of the anions at the air/water interface of the electrolyte aqueous solution ought to be about two orders of magnitude less than that predicted by the MD simulation results.[4]

Unless some other unknown physical mechanism is introduced, neutrality at the interface is the key to keep the EFISHG and the EFISFG term negligible. This leads to the conclusion of a much weaker electric double layer due to the preferable adsorption of the anions at the electrolyte solution interface. However, this does not imply that the anion concentration cannot be as high as MD simulation predicts, as long as the interface charge neutrality is maintained with a similar amount of cations.

The weak electric double layer at the NaF, NaCl and NaBr solution interfaces might also be responsible for the less significant specific anion effect on the air/water interface than that at the polymer/water interfaces.[101] Nevertheless, we would like to point out the fact that the sequence of the increase of the interfacial water thickness of these three salts still followed the order of the Hofmeister series.[101,102]

V. Conclusions

In this report, specific ion effects on the nonlinear optical response from the water molecules at three air/sodium halide solution interfaces are measured using the surface non-resonant SHG. Procedures have been developed to monitor and remove the impurities in the salt solution samples to ensure measurement of small changes in the SHG signal. Quantitative polarization analysis of the measured SHG data indicated that the average orientation of the interfacial water molecules changed only slightly around 40° with the increase of the bulk concentration of the three sodium halides, namely NaF, NaCl and NaBr, from that of the neat air/water interface. The observed significant SHG signal increase with the bulk salt concentration is attributed to the overall increase of the thickness of the interfacial water molecules, following the order of NaBr $>$ NaCl $\approx$ NaF. The absence of the electric-field-induced SHG (EFISHG) effect indicated that the electric double layer at the salt aqueous solution interface is much weaker than as predicted from the molecular dynamics (MD) simulations. Nevertheless, these results provided quantitative data to the specific anion effects on the interfacial water molecules of the electrolyte aqueous solution, not only for the larger and more polarizable Br^- anion, but also for the smaller and less polarizable F^- and Cl^- anions.

Unlike the SFG-VS, non-resonant SHG is not sensitive to distinguish the different hydrogen bonded water species at the interface. Therefore, the non-resonant SHG is ideal for probing the whole interfacial water molecular layer thickness. The studies with the non-resonant SHG on other electrolyte aqueous solution interfaces are also expected. Comparison of the SHG and the SFG-VS studies shall provide both the overall and specific information about the interfacial water molecular structure at the electrolyte aqueous solution. Comparison of the SHG and other theoretical simulation methods or experimental techniques also need to be further explored. With these studies, the role and the underline principles of the increased thickness or depth of the interfacial water molecular layer might be finally revealed.

Acknowledgements

HTB thanks helpful discussions from Wen-kai Zhang and Desheng Zheng. HTB also thanks An-an Liu for providing the quantum calculation of the water hyperpolarizability. HFW thanks the support by the Natural Science Foundation of China (NSFC, No. 20425309, No. 20533070, No. 20773143) and the Ministry of Science and technology of China (MOST No. 2007CB815205). YG thanks the support by the Natural Science Foundation of China (NSFC, No. 20673122).

References

1. S. Durand-Vidal, J.-P. Simonin and P. Turq, *Electrolytes at Interfaces*, Kluwer Academic, Boston, 2000.
2. Y. R. Shen and V. Ostroverkhov, *Chem. Rev.*, 2006, **106**, 1140.
3. S. Gopalakrishnan, D. F. Liu, H. C. Allen, M. Kuo and M. J. Shultz, *Chem. Rev.*, 2006, **106**, 1155.
4. P. Jungwirth and D. J. Tobias, *Chem. Rev.*, 2006, **106**, 1259.
5. T. M. Chang and L. X. Dang, *Chem. Rev.*, 2006, **106**, 1305.
6. P. B. Petersen and R. J. Saykally, *Annu. Rev. Phys. Chem.*, 2006, **57**, 333.
7. B. C. Garrett, *Science*, 2004, **303**, 1146.
8. D. F. Liu, G. Ma, L. M. Levering and H. C. Allen, *J. Phys. Chem. B*, 2004, **108**, 2252.
9. E. A. Raymond and G. L. Richmond, *J. Phys. Chem. B*, 2004, **108**, 5051.
10. E. M. Knipping, M. J. Lakin, K. L. Foster, P. Jungwirth, D. J. Tobias, R. B. Gerber, D. Dabdub and B. J. Finlayson-Pitts, *Science*, 2000, **288**, 301.
11. M. Mucha, T. Frigato, L. M. Levering, H. C. Allen, D. J. Tobias, L. X. Dang and P. Jungwirth, *J. Phys. Chem. B*, 2005, **109**, 7617.
12. K. L. Foster, R. A. Plastridge, J. W. Bottenheim, P. B. Shepson, B. J. Finlayson-Pitts and C. W. Spicer, *Science*, 2001, **291**, 471.
13. A. Laskin, D. J. Gaspar, W. H. Wang, S. W. Hunt, J. P. Cowin, S. D. Colson and B. J. Finlayson-Pitts, *Science*, 2003, **301**, 340.
14. S. Ghosal, J. C. Hemminger, H. Bluhm, B. S. Mun, E. L. D. Hebenstreit, G. Ketteler, D. F. Ogletree, F. G. Requejo and M. Salmeron, *Science*, 2005, **307**, 563.
15. P. Jungwirth and D. J. Tobias, *J. Phys. Chem. B*, 2001, **105**, 10468.
16. P. Jungwirth and D. J. Tobias, *J. Phys. Chem. B*, 2002, **106**, 6361.
17. L. X. Dang, *J. Phys. Chem. B*, 2002, **106**, 10388.
18. P. Jungwirth and B. Winter, *Annu. Rev. Phys. Chem.*, 2008, **59**, 343.
19. D. J. Tobias and J. C. Hemminger, *Science*, 2008, **319**, 1197.

20. I. Langmuir, *J. Am. Chem. Soc.*, 1917, **39**, 1848.
21. L. Onsager and N. N. T. Samaras, *J. Chem. Phys.*, 1934, **2**, 528.
22. A. W. Adamson, *Physical Chemistry of Surfaces*, John Wiley & Sons, New York, 5th edn, 1990.
23. V. S. Markin and A. G. Volkov, *J. Phys. Chem. B*, 2002, **106**, 11810.
24. G. Markovich, R. Giniger, M. Levin and O. Cheshnovsky, *J. Chem. Phys.*, 1991, **95**, 9416.
25. G. Markovich, S. Pollack, R. Giniger and O. Cheshnovsky, *J. Chem. Phys.*, 1994, **101**, 9344.
26. L. Perera and M. L. Berkowitz, *J. Chem. Phys.*, 1991, **95**, 1954.
27. L. X. Dang and D. E. Smith, *J. Chem. Phys.*, 1993, **99**, 6950.
28. L. Perera and M. L. Berkowitz, *J. Chem. Phys.*, 1994, **100**, 3085.
29. J. H. Hu, Q. Shi, P. Davidovits, D. R. Worsnop, M. S. Zahniser and C. E. Kolb, *J. Phys. Chem.*, 1995, **99**, 8768.
30. V. Padmanabhan, J. Daillant, L. Belloni, S. Mora, M. Alba and O. Konovalov, *Phys. Rev. Lett.*, 2007, **99**, 086105.
31. K. B. Eisenthal, *Chem. Rev.*, 1996, **96**, 1343.
32. P. B. Miranda and Y. R. Shen, *J. Phys. Chem. B*, 1999, **103**, 3292.
33. P. B. Petersen, J. C. Johnson, K. P. Knutsen and R. J. Saykally, *Chem. Phys. Lett.*, 2004, **397**, 46.
34. P. B. Petersen and R. J. Saykally, *Chem. Phys. Lett.*, 2004, **397**, 51.
35. P. B. Petersen and R. J. Saykally, *J. Phys. Chem. B*, 2005, **109**, 7976.
36. P. B. Petersen, R. J. Saykally, M. Mucha and P. Jungwirth, *J. Phys. Chem. B*, 2005, **109**, 10915.
37. P. B. Petersen and R. J. Saykally, *J. Am. Chem. Soc.*, 2005, **127**, 15446.
38. P. B. Petersen and R. J. Saykally, *J. Phys. Chem. B*, 2006, **110**, 14060.
39. C. Schnitzer, S. Baldelli and M. J. Shultz, *J. Phys. Chem. B*, 2000, **104**, 585.
40. P. Viswanath and H. Motschmann, *J. Phys. Chem. C*, 2007, **111**, 4484.
41. P. Viswanath and H. Motschmann, *J. Phys. Chem. C*, 2008, **112**, 2099.
42. E. Sloutskin, J. Baumert, B. M. Ocko, I. Kuzmenko, A. Checco, L. Tamam, E. Ofer, T. Gog, O. Gang and M. Deutsch, *J. Chem. Phys.*, 2007, **126**, 054704.
43. D. Clifford and D. J. Donaldson, *J. Phys. Chem. A*, 2007, **111**, 9809.
44. Q. Du, R. Superfine, E. Freysz and Y. R. Shen, *Phys. Rev. Lett.*, 1993, **70**, 2313.
45. C. Raduge, V. Pflumio and Y. R. Shen, *Chem. Phys. Lett.*, 1997, **274**, 140.
46. M. J. Shultz, C. Schnitzer, D. Simonelli and S. Baldelli, *Int. Rev. Phys. Chem.*, 2000, **19**, 123.
47. L. M. Levering, M. R. Sierra-Hernandez and H. C. Allen, *J. Phys. Chem. C*, 2007, **111**, 8814.
48. X. Wei and Y. R. Shen, *Phys. Rev. Lett.*, 2001, **86**, 4799.
49. G. L. Richmond, *Chem. Rev.*, 2002, **102**, 2693.
50. W. Gan, D. Wu, Z. Zhang, R. R. Feng and H. F. Wang, *J. Chem. Phys.*, 2006, **124**, 114705.
51. W. Gan, D. Wu, Z. Zhang, Y. Guo and H. F. Wang, *Chin. J. Chem. Phys.*, 2006, **19**, 20.
52. N. Ji, V. Ostroverkhov, C. S. Tian and Y. R. Shen, *Phys. Rev. Lett.*, 2008, **100**, 096102.
53. Y. R. Shen, *Annu. Rev. Phys. Chem.*, 1989, **40**, 327.
54. W. K. Zhang, D. S. Zheng, Y. Y. Xu, H. T. Bian, Y. Guo and H. F. Wang, *J. Chem. Phys.*, 2005, **123**, 224713.
55. W. K. Zhang, H. F. Wang and D. S. Zheng, *Phys. Chem. Chem. Phys.*, 2006, **8**, 4041.
56. Y. Rao, Y. S. Tao and H. F. Wang, *J. Chem. Phys.*, 2003, **119**, 5226.
57. Y. R. Shen, *Nature*, 1989, **337**, 519.
58. H. F. Wang, W. Gan, R. Lu, Y. Rao and B. H. Wu, *Int. Rev. Phys. Chem.*, 2005, **24**, 191.
59. X. W. Zhuang, P. B. Miranda, D. Kim and Y. R. Shen, *Phys. Rev. B*, 1999, **59**, 12632.
60. G. L. Richmond, J. M. Robinson and V. L. Shannon, *Prog. Surf. Sci.*, 1988, **28**, 1.
61. K. B. Eisenthal, *Acc. Chem. Res.*, 1993, **26**, 636.
62. T. G. Zhang, C. H. Zhang and G. K. Wong, *J. Opt. Soc. Am. B*, 1990, **7**, 902.
63. S. W. Ong, X. L. Zhao and K. B. Eisenthal, *Chem. Phys. Lett.*, 1992, **191**, 327.
64. X. L. Zhao, S. W. Ong and K. B. Eisenthal, *Chem. Phys. Lett.*, 1993, **202**, 513.
65. H. F. Wang, X. L. Zhao and K. B. Eisenthal, *J. Phys. Chem. B*, 2000, **104**, 8855.
66. G. L. Gaines, *Insoluble Monolayers at Liquid-Gas Interfaces*, Wiley, New York, 1965.
67. S. McLaughlin, *Annu. Rev. Biophys. Biophys. Chem.*, 1989, **18**, 113.
68. G. Ahn-Ercan, H. Krienke and W. Kunz, *Curr. Opin. Colloid Interface Sci.*, 2004, **9**, 92.
69. D. P. Shelton, *Chem. Rev.*, 1994, **94**, 3.
70. Unpublished data.
71. Y. Rao, X. M. Guo and H. F. Wang, *J. Phys. Chem. A*, 2004, **108**, 7987.
72. R. Lu, W. Gan, B. H. Wu, H. Chen and H. F. Wang, *J. Phys. Chem. B*, 2004, **108**, 7297.
73. R. Lu, W. Gan, B. H. Wu, Z. Zhang, Y. Guo and H. F. Wang, *J. Phys. Chem. B*, 2005, **109**, 14118.
74. H. Chen, W. Gan, R. Lu, Y. Guo and H. F. Wang, *J. Phys. Chem. B*, 2005, **109**, 8064.
75. X. L. Zhao, M. C. Goh, S. Subrahmanyan and K. B. Eisenthal, *J. Phys. Chem.*, 1990, **94**, 3370.
76. M. C. Goh, J. M. Hicks, K. Kemnitz, G. R. Pinto, K. Bhattacharyya, K. B. Eisenthal and T. F. Heinz, *J. Phys. Chem.*, 1988, **92**, 5074.
77. A. J. Fordyce, W. J. Bullock, A. J. Timson, S. Haslam, R. D. Spencer-Smith, A. Alexander and J. G. Frey, *Mol. Phys.*, 2001, **99**, 677.
78. J. G. Frey, *Chem. Phys. Lett.*, 2000, **323**, 454.
79. A. A. T. Luca, P. Hebert, P. F. Brevet and H. H. Girault, *J. Chem. Soc., Faraday Trans.*, 1995, **91**, 1763.
80. D. R. Lide, *CRC Handbook of Chemistry and Physics*, CRC Press, 85th edn, 2005.
81. M. A. Wilson, A. Pohorille and L. R. Pratt, *J. Phys. Chem.*, 1987, **91**, 4873.
82. B. Yang, D. E. Sullivan, B. Tjipto-Margo and C. G. Gray, *J. Phys.: Condens. Matter*, 1991, **3**, F109.
83. I. Benjamin, *Phys. Rev. Lett.*, 1994, **73**, 2083.
84. N. A. M. Besseling and J. Lyklema, *J. Phys. Chem.*, 1994, **98**, 11610.
85. R. S. Taylor, L. X. Dang and B. C. Garrett, *J. Phys. Chem.*, 1996, **100**, 11720.
86. V. P. Sokhan and D. J. Tildesley, *Mol. Phys.*, 1997, **92**, 625.
87. C. Fradin, A. Braslau, D. Luzet, D. Smilgies, M. Alba, N. Boudet, K. Mecke and J. Daillant, *Nature*, 2000, **403**, 871.
88. A. Morita and J. T. Hynes, *Chem. Phys.*, 2000, **258**, 371.
89. A. Perry, H. Ahlborn, B. Space and P. B. Moore, *J. Chem. Phys.*, 2003, **118**, 8411.
90. I-F. W. Kuo and C. J. Mundy, *Science*, 2004, **303**, 658.
91. K. Jaqaman, K. Tuncay and P. J. Ortoleva, *J. Chem. Phys.*, 2004, **120**, 926.
92. P. A. Franken and J. F. Ward, *Rev. Mod. Phys.*, 1963, **35**, 23.
93. C. A. Dailey, B. J. Burke and G. J. Simpson, *Chem. Phys. Lett.*, 2004, **390**, 8.
94. Z. R. Tang, M. Cavanagh and J. F. McGilp, *J. Phys.: Condens. Matter*, 1993, **5**, 3791.
95. M. in het Panhuis and R. W. Munn, *J. Chem. Phys.*, 2000, **112**, 6763.
96. M. in het Panhuis and R. W. Munn, *J. Chem. Phys.*, 2000, **113**, 10691.
97. W. M. B. Yunus and A. B. Rahman, *Appl. Opt.*, 1988, **27**, 3341.
98. G. J. Simpson and K. L. Rowlen, *J. Am. Chem. Soc.*, 1999, **121**, 2635.
99. G. J. Simpson and K. L. Rowlen, *Anal. Chem.*, 2000, **72**, 3399.
100. G. J. Simpson and K. L. Rowlen, *Anal. Chem.*, 2000, **72**, 3407.
101. X. Chen, T. L. Yang, S. Kataoka and P. S. Cremer, *J. Am. Chem. Soc.*, 2007, **129**, 12272.
102. F. Hofmeister, *Arch. Exp. Pathol. Pharmakol.*, 1888, **24**, 247.